PHYSICAL REVIEW E, VOLUME 65, 010702(R)

Photonic band structure of highly deformable self-assembling systems

P. A. Bermel and M. Warner
Cavendish Laboratory, University of Cambridge, Madingley Road, Cambridge CB3 0HE, United Kingdom
(Received 28 March 2001; published 14 December 2001)

We calculate the photonic band structure at normal incidence of highly deformable, self-assembling systems—cholesteric elastomers subjected to external stress. Cholesteric elastomers display brilliantly colored reflections and lasing owing to gaps in their photonic band structure. This band structure has been shown to vary sensitively with strain in both theory and experiment. New gaps open up and all gaps shift in frequency. We predict a different "total" band gap for all polarizations in the vicinity of the previously observed de Vries band gap, which is only for one polarization.

DOI: 10.1103/PhysRevE.65.010702 PACS number(s): 61.30.−v, 81.40.Jj, 42.70.Qs

Photonic band-gap (PBG) materials offer a new approach to the manipulation of light that depends on the structure rather than the atomic or molecular properties of materials. These materials have two unique properties that has spurred interest in their design, namely, the localization of light [1] and modification of the spontaneous emission spectrum from atoms and molecules [2]. Several approaches have been taken to manufacture PBG materials. Yablonovitch constructed an fcc photonic crystal by drilling holes into a dielectric medium [3]. Later, Ozbay and co-workers designed a picket fence structure that is assembled by stacking two-dimensional layers [4].

Recently, there has been an increased interest in self-assembling PBG systems due to their relative ease of manufacture for operation at optical and near-infrared wavelengths. Several examples include air holes in a titania matrix [5], copolymer-homopolymer films that form lamellar structures [6], thin films of poly-(methyl-methacrylate) infilled with SnS_2 [7], and cholesteric liquid crystals (CLCs) [8–10].

One of the most promising applications of photonic band-gap materials is in low-threshold lasing. Yablonovitch and Gmitter [3] first predicted that the lasing threshold would be decreased by introducing a defect into an otherwise perfect photonic material. Since spontaneous emission is suppressed in the bulk, excitation would not be drained by any emission into nonlasing modes. Such low-threshold lasing has recently been observed in two-dimensional photonic crystals [11]. Alternatively, one can design lasers that take advantage of the enhanced dwell time associated with the band edge divergence of the density of states [12]. Experimentally, this band-edge lasing has been observed in CLC's [9] and cholesteric elastomers (CE's) [10], for reasons we shall relate to the band structures we predict.

A CLC has local orientational ordering along a director **n**, which rotates as a periodic function of distance along the pitch axis *z*. The director of an ideal CLC advances uniformly, tracing out a helix of pitch p_0. The pitch can be adjusted to match the wavelength of visible light, whereupon a number of spectacular optical effects are observed experimentally and explained theoretically [8]. In particular, in experiments conducted at normal incidence, circularly polarized light that twists in the same sense as the helix is reflected with its original polarization, while circularly polarized light that twists in the opposite sense is transmitted unchanged. Normal incidence has been of prime concern since the optical response of such twisting nematic media is the basis of liquid crystal (LC) display technology. A CLC can be considered locally uniaxial, with a dielectric permittivity $\epsilon_\parallel$ along **n** and $\epsilon_\perp$ perpendicular to **n**. By solving Maxwell's equations in a rotating frame, de Vries found a single band gap in the photonic structure of an ideal CLC at normal incidence [8].

The calculations we present on CE's point to different phenomena and different applications, not possible in existing photonics and hitherto unsuspected in the liquid crystal field. For instance, we find multiple gaps, some not at the zone edges, in contrast to classical CLC's. We also observe gaps for light of the opposite handedness to the underlying helix, again unexpected in classical CLC systems. At some points the gaps for both polarizations overlap, giving a total gap of significance when polarization control is required. Our systems are highly deformable (to many 100s%) and we shall find shifts in the (developing) band structure that can be large and that are experimentally confirmed [10,13]. Existent photonic media typically have piecewise variation of an isotropic refractive index in going between a matrix and its inclusions. In one theoretical calculation, nematic liquid crystals were used to fill an inverse opal structure [14]; however, the problem was readily transformed to the previous problem by a uniform rotation of the coordinate axes. By contrast, CLC's have a continuous variation of the principal axes of birefringence, which corresponds to a continuously rotating coordinate frame. The principal axes guide the waves along a generally nontrivial, periodic path and give rise to sharply different behaviors for each polarization. Polarization effects are thus very subtle and become more so for oblique incidence, which we consider in greater detail elsewhere. Control of polarization is at the heart of LC and optical devices; we thus view this work as a first step toward different classes of photonic solids with deformable, tunable band structures for different applications.

CE's can be made by crosslinking cholesteric polymer liquid crystals [13]. Defect-free monodomain rubber strips tens of centimeters long display spectacular optical effects, viz. large changes in the frequencies of reflection and lasing [10] in response to imposed mechanical strains that couple to director orientation (Fig. 1). These strips can be thick and are

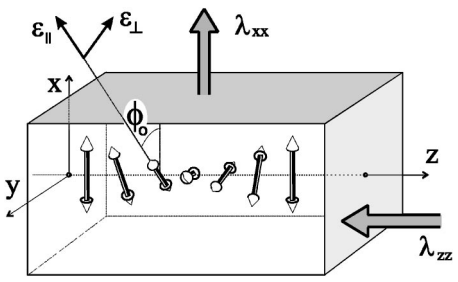

FIG. 1. A CE showing the initially helical director distribution, $\phi_0(z)$. Elongation λ_{xx} is applied perpendicular to the pitch axis that contracts by λ_{zz}. The dielectric tensor is represented in its local principal frame by $\epsilon_\parallel$ and $\epsilon_\perp$.

oriented not by surface anchoring as in liquids, but by interaction between local directors and the rubber matrix.

Elongations $\lambda \equiv \lambda_{xx}$, applied perpendicularly to the pitch axis (see Fig. 1) are predicted to coarsen the initially helical director structure, given by $\phi_0 = q_0 z$ (where ϕ is the angle the director makes with the x axis), to one dominated by regions of slowly varying angles, separated by increasingly sharp twist walls [15], see Fig. 2.

At a critical $\lambda = \lambda_c$, the walls become thermodynamically unstable and the director experiences periodic oscillations about $\phi = 0$ that diminish with increasing λ. There are attendant contractions perpendicular to the stretch. The pitch shrinks affinely [10] with the matrix. In the small stretching limit ($\lambda \to 1$), the pitch varies as $p = p_0 \lambda^{-2/7}$ and the first reciprocal lattice vector goes as $q = q_0 \lambda^{2/7}$. Thus, the band structure changes upon extension because of two factors, the dilation of the reciprocal space and the change in the modulation character of the dielectric tensor along the pitch axis, $\underline{\underline{\epsilon}}(z)$. These changes can be very large.

I. THEORY

Maxwell's equations yield [16]

$$\left(\frac{\omega}{c}\right)^2 \mathbf{H} = \nabla \times [\underline{\underline{\epsilon}}(z)^{-1} (\nabla \times \mathbf{H})]. \tag{1}$$

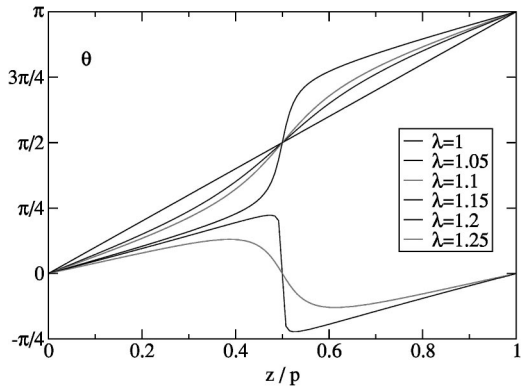

FIG. 2. Modification of director distribution, $\phi(\tilde{z})$ by an x deformation λ. The dielectric tensor's principal frame follows $\phi(\tilde{z})$, helix distortions induce band-structure changes.

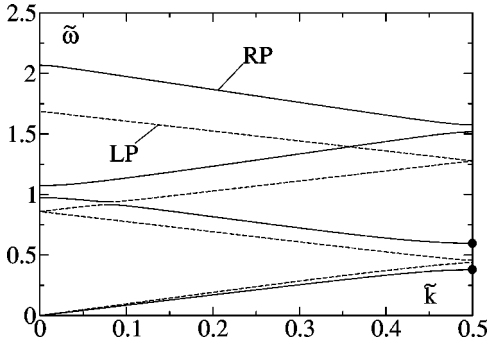

FIG. 3. For $\lambda = 1.1 < \lambda_c$, two differences from the de Vries case are observed: (1) additional band gaps are created at higher zone boundaries for the RP branch and (2) band gaps are also observed for the previously uninteresting LP branch, albeit much smaller than the RP gaps. The single gap in the de Vries case is approximately that marked by dots.

For normal incidence, along the z axis, the magnetic field $\mathbf{H}$ is transverse and exists wholly in the xy plane. We thus suppress the z components in the inverse dielectric tensor, given by

$$\begin{pmatrix} \epsilon_\parallel^{-1} & 0 \\ 0 & \epsilon_\perp^{-1} \end{pmatrix}$$

in its principal frame [oriented at angle $\phi(z)$ to x, Fig. 1]. ∇ is only $(d/dz)\hat{z}$.

We apply Bloch's theorem to decompose $\mathbf{H}$ into plane wave components [16], so that

$$\mathbf{H} = \sum_{G,\gamma} h_{(G\gamma)} \hat{e}_\gamma e^{i(k+G)z}, \tag{2}$$

where the unit vectors are $\gamma = \{1,2\}$, $\hat{e}_1 = \hat{x}$, and $\hat{e}_2 = \hat{y}$, and the reciprocal lattice vector $\mathbf{G} = 2nq\hat{z}$, for n integer. This procedure yields a matrix equation that reduces to a dimensionless form, lengths transform according to $z \to \tilde{z} = zq/2\pi$, wave vectors go as $k \to \tilde{k} = k/q$, reciprocal lattice vectors $G \to 2n$, frequencies go as $\omega \to \tilde{\omega} = \omega/(cq\sqrt{a})$ and $\underline{\underline{\epsilon}}^{-1} \to \underline{\underline{\epsilon}}^{-1}/a$ where $a = \frac{1}{2}[(1/\epsilon_\parallel) + (1/\epsilon_\perp)]$. This reduction is important for the proper interpretation of the shifts of band structure with elongation in Figs. 3 and 4. Since $q = q_o \lambda^{2/7}$ changes with λ, so do ω and k.

Equation (1) then assumes the form $\underline{\underline{A}}^{\tilde{k}}_{(n\gamma),(n\gamma)'} h_{(n\gamma)'} = \tilde{\omega}^2 h_{(n\gamma)}$. $\underline{\underline{A}}^{\tilde{k}}$ thus determines the photonic band structure of a CLC. It depends on the reduced inverse dielectric tensor at arbitrary z and thus at angle $\phi = \phi(z)$,

$$\underline{\underline{\epsilon}}^{-1}(z) = \underline{\underline{1}} - \alpha\{[\cos(2\phi)]\underline{\underline{\sigma}}_z + [\sin(2\phi)]\underline{\underline{\sigma}}_x\}, \tag{3}$$

where $\alpha \equiv (\epsilon_\parallel - \epsilon_\perp)/(\epsilon_\parallel + \epsilon_\perp)$ follows the notation of de Vries [8], and the $\underline{\underline{\sigma}}_i$ are the Pauli spin matrices.

One can then show that in γ space, $\underline{\underline{A}}^{\tilde{k}}$ is given by

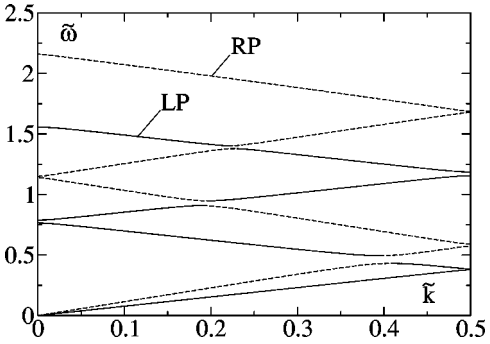

FIG. 4. For $\lambda = 1.3 > \lambda_c$, substantial divergence from the de Vries dispersion relation is observed. A full band gap away from the Brillouin zone boundary is observed, as well as several anticrossings between branches.

$$\underline{\underline{A}}^{\tilde{k}}_{n,n'} = (\tilde{k}+n)^2 \delta_{n,n'} \underline{\underline{1}} + \alpha(\tilde{k}+n)(\tilde{k}+n') \times (c_{n'-n}\underline{\underline{\sigma}}_z + s_{n'-n}\underline{\underline{\sigma}}_x), \quad (4)$$

where $s_{n'-n}$ and $c_{n'-n}$ are the Fourier coefficients of $\sin(2\phi)$ and $\cos(2\phi)$, respectively,

$$s_n \equiv \int_0^{1/2} d\tilde{z} \sin[2\phi(\tilde{z})] \exp(-4\pi i n \tilde{z})$$

and c_n, similarly.

The undeformed director angles $\phi(\tilde{z})$ are $\phi_0 = 2\pi\tilde{z}$. On an x strain λ, accompanied by relaxation $\lambda_{yy}(\lambda)$ assumed to be uniform and determined by energy minimization, the principal frame orientation is given by [15]

$$\tan(2\phi) = \frac{2\lambda\lambda_{yy}(r-1)\sin(4\pi\tilde{z})}{(r-1)(\lambda^2+\lambda_{yy}^2)\cos(4\pi\tilde{z}) + (r+1)(\lambda^2-\lambda_{yy}^2)},$$

where r is the shape anisotropy of the polymers underlying the nematic phase. See Fig. 2 for $\phi(\tilde{z})$ for various $\delta = \lambda - 1$. From $\tan(2\phi)$, one can easily obtain $\sin(2\phi)$ and $\cos(2\phi)$, and thus, $s_{n'-n}$ and $c_{n'-n}$.

Numerical diagonalization of the matrix $\underline{\underline{A}}^{\tilde{k}}_{(n\lambda),(n\lambda)'}$ at a range of $\tilde{k}$ yields a dispersion relation $\tilde{\omega}(\tilde{k})$, along with eigenvectors giving the character of each solution. In general, the eigenvectors are elliptically polarized inside the CLC medium, with semimajor and semiminor axes corresponding at each point to the local principal axes of the dielectric tensor, and nearly circularly polarized *in vacuo* [8]. We take $\epsilon_\parallel = 3$ and a depressed value $\epsilon_\perp = 1.2$ throughout, simply for readability.

At small $\tilde{k} \ll 1$, the dispersion relation for an ideal CLC (i.e., $\lambda = \lambda_{yy} = 1$) is linear, corresponding to nondispersive waves, with a simple effective refractive index $m = \sqrt{(\epsilon_\perp + \epsilon_\parallel)/2}$, suggesting that both modes effectively experience the same, homogeneous medium at long wavelengths. This small $\tilde{k}$ behavior is initially retained in the strain-modified band structures, see Fig. 3.

At $\tilde{k} = 1$, branch, denoted by RP in Figs. 3 and 4, whose polarization rotates in the same sense as the helix *in vacuo* develops the de Vries gap [8]. The eigenmodes of this branch at the zone boundary are linearly polarized inside the CLC medium. The lower band's electric vector points along $\mathbf{n}(\mathbf{r})$, the upper band's perpendicularly to $\mathbf{n}(\mathbf{r})$, in the xy plane. The other branch, denoted by LP, however, cannot split analogously, since its polarization *in vacuo* rotates in a sense opposite to the helix. This is qualitatively similar to the major gap in the distorted band structure, marked with dots at $\tilde{k} = 1$ in Fig. 3. Furthermore, no gaps are observed for $\tilde{k} > 1$, because band gaps are created only when degenerate energy states are linked by nonzero matrix elements. Since in the de Vries case, there are only two harmonic components of equal and opposite frequencies, only the matrix elements linking the two lowest energy states on either side of the first Brillouin zone boundary are nonvanishing.

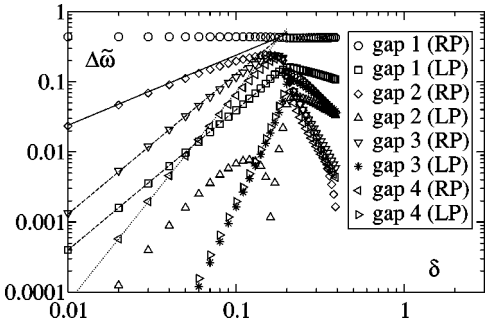

FIG. 5. Scaling of the first to fourth gap sizes of a CE with δ. The points represent numerical data, the straight lines, predictions from perturbation theory (assuming a scaling form for c_n and s_n).

We now stretch CE's with $r = 1.9$ for definiteness, which gives a $\lambda_c \approx r^{2/7} \approx 1.2$ [15]. Figure 3 shows the dispersion relation for an elongation $\lambda = 1.1 < \lambda_c$. Since the first Brillouin zone boundary is at $\tilde{k} = 1$, band gaps may occur at $k = nq_0\lambda^\beta$, for integer $n \neq 0$, with $\beta = 2/7$. This corresponds to a shift in color and in lasing frequency, as observed in CE's [10,13], toward the ultraviolet.

For $\lambda \geqslant \lambda_c$, there is a qualitative change in the behavior of the director, $\phi(z)$ (see Fig. 2), and thus a qualitative change in the band structure. Additionally, the scaling behavior of $\lambda_{zz}(\lambda) = \lambda^{-\beta}$ changes [15] from $\beta = 2/7$, in the limit of small stretching ($\lambda \sim 1$), to $\beta = 1/2$ for $\lambda > \lambda_c$, the classical exponent for isotropic CE's. Figure 4 shows the dispersion relation for a stretch $\lambda = 1.3 > \lambda_c$.

We now analyze the gap structures that open up in the stretched case, $\lambda > 1$. The elastic strain, $\delta \equiv \lambda - 1$, is the perturbation parameter modifying the perfect helical structure. Whereas before, $c_{\pm 1} = 1/2$ and $c_n = 0$, otherwise, we now have nonzero values for $c_{\pm n}$ that scale as δ^{n-1} for $n > 1$ and $\delta \ll 1$; $c_{\pm 1} = 1 - O(\delta^2)$ and $c_0 \sim \delta$. Applying degenerate perturbation theory, we eliminate all matrix elements in $\underline{\underline{A}}^{n_0}_{(n\lambda),(n\lambda)'}$ except for those linking the degenerate energy states, and predict that the gaps for the interesting polarization in the de Vries case will scale with the magnitude of the off-diagonal elements, given by c_{n_0}. The first order (de Vries) gap will be approximately constant, the second order gap (first new gap) will grow as δ, the third order gap will grow as δ^2, and so on, see Fig. 5. More precisely, at the first

order gap, $\tilde{\omega}^2 = 1 \pm \alpha(c_1 \pm \sqrt{c_0^2 - s_1^2})$, since $s_0 = 0$. As a result, we also predict that the opposite polarization will now have a nonzero gap that scales as δ^2. That tells us that a *full* photonic band gap will be created at $\tilde{k} = 1$ as we perturb our helix by transverse elongation, and that its size will scale as δ^2, the size of the much smaller gap of opposite polarization, see Figs. 3 and 5.

Of experimental interest is the *in vacuo* wavelength, Λ, of the light corresponding to a given $\tilde{\omega}$ on the dispersion relation, particularly at the gaps. The definitions below Eq. (2) give $\Lambda = p_0/(\tilde{\omega}\sqrt{a}\lambda^{2/7})$. Pitches p_0 typically give a band in the visible so the initial wavelengths are $\Lambda_0 = p_0/\sqrt{a} \sim 500$ nm at $\tilde{\omega} = \lambda = 1$, which allows us to write $\Lambda = \Lambda_0/(\tilde{\omega}\lambda^{2/7})$. Likewise the first order de Vries gap is given by $\Delta\Lambda \approx \Lambda_0/\lambda^{2/7}\alpha$. The higher order gaps of the same polarization will have widths of $\Delta\Lambda_n \approx C\Lambda_0\delta^{n-1}/(n\lambda^{2/7})$, where C is a prefactor of order unity that will depend on r and α. For example, the second order gap in a rubber with $r = 1.9$, $\alpha = 0.43$, and $\delta = 0.1$, the gap will be $\Delta\Lambda_2 \approx 0.045\Lambda_0$. For $\Lambda_0 \approx 800$ nm, that implies a stop band for the light with a circular polarization of the same sense as the helix will be observed for $\Lambda = 362$ nm to $\Lambda = 398$ nm.

Finally, a note about oblique incidence in CE's. By symmetry, we expect that the magnetic field must have the same magnitude at all points for a given z, and only differ by a phase. That lets us generalize the $\boldsymbol{H}$ vector for normal incidence, Eq. (2), by $\mathbf{k} \rightarrow \mathbf{k}' = k_\perp \hat{\rho} + k_\parallel \hat{z}$ and $\hat{e}_\gamma \rightarrow \hat{e}'_{(G\gamma)}$. Our preliminary findings indicate that for a constant k', the stop bands shift upwards as we increase the angle of incidence from zero, which implies that refraction out of a normally incident beam path is forbidden for modes just above the stop band. That observation provides a mechanism to explain the spatial coherence of the light produced by dye-doped pumped lasers based on CLC's and CE's [9,10].

II. CHOLESTERIC LIQUIDS

Apply a magnetic field $\boldsymbol{H}$ along the y direction. A CLC has an anisotropic susceptibility $\chi_a = \chi_\parallel - \chi_\perp$. The helix untwists (increasing the period) and coarsens [17] until the energy gain from aligning with the field balances the Frank penalty for deviations from the original structure. The director orientations coarsen, as in Fig. 2, but with the z coordinate being reduced to $\tilde{z}$ by a *lengthening* period. At a critical field $H_c = (\pi q_0/2)\sqrt{K_{22}/\chi_a}$, where K_{22} is the Frank twist elastic constant, the period diverges logarithmically as the entire sample aligns with the external field [17]. For typical cholesteric liquids with a pitch of 20μm, $H_c = 15\,000$ G, and $E_c = 50$ sV/cm [17]. Differences from CEs under strain are detailed in [15].

The optical implications of coarsening were investigated by Meyer and co-workers [18]. We find the Fourier coefficients describing the twist of the cholesteric liquid to scale just as the coefficients describing CE's for $\lambda < \lambda_c$. One can use the results for the CE case for a cholesteric liquid under the transformation $\delta \rightarrow \tilde{h}^2$. The dispersion relations are qualitatively the same as in Fig. 3. The width and scaling of the gaps created resemble those of Fig. 5, but with all effects ending abruptly at $\tilde{h} = 1$.

III. CONCLUSIONS

An entirely different type of photonic material has been described and characterized. Not only is it self-assembling and easily available as large, defect-free single crystals, but it is highly deformable. Earlier descriptions [15,17] of its modified periodic dielectric structure have been used as the basis for calculating its band structure. New gaps arise and their widths scale in a well-understood fashion with the stretch applied to the material or the strength of the external field. The midgap frequencies shift position by large amounts comparable to their initial values.

ACKNOWLEDGMENTS

We thank A. Genack and P. Palffy-Muhoray for introducing us to lasing in cholesterics, and acknowledge valuable discussions with E. M. Terentjev, Y. Mao, H. Finkelmann, S. T. Kim, W. Stille, S. Shiyanovskii, P. D. Haynes, P. B. Littlewood, and S. Johnson.

[1] S. John, Phys. Rev. Lett. **58**, 2486 (1987).
[2] M.D. Tocci *et al.*, Phys. Rev. A **53**, 2799 (1996).
[3] E. Yablonovitch *et al.*, Phys. Rev. Lett. **63**, 1950 (1989).
[4] E. Ozbay *et al.*, Phys. Rev. B **50**, 1945 (1994).
[5] J.E. Wijnhoven and W.L. Vos, Science **281**, 802 (1998).
[6] A. Urbas *et al.*, Macromolecules **32**, 4748 (1999).
[7] M. Muller *et al.*, Adv. Mater. **12**, 1499 (2000).
[8] H. de Vries, Acta Crystallogr. **4**, 219 (1951).
[9] V.I. Kopp *et al.*, Opt. Lett. **23**, 1707 (1998); B. Taheri *et al.*, in *Proceedings of the ALCOM Symposium* (Cuyahoga Falls, Ohio, 1999).
[10] H. Finkelmann, S. T. Kim, A. Muñoz, P. Palffy-Muhoray, and B. Taheri, Adv. Mater. **13**, 1069 (2001).
[11] O. Painter *et al.*, Science **284**, 1819 (1999).
[12] J.P. Dowling *et al.*, J. Appl. Phys. **75**, 1896 (1994).
[13] S.T. Kim and H. Finkelmann, Macromol. Rapid Commun. **22**, 429 (2001).
[14] K. Busch and S. John, Phys. Rev. Lett. **83**, 967 (1999).
[15] M. Warner *et al.*, Phys. Rev. Lett. **85**, 2320 (2000).
[16] R.D. Meade *et al.*, Phys. Rev. B **48**, 8434 (1993).
[17] R.B. Meyer, Appl. Phys. Lett. **12**, 281 (1968); P.G. de Gennes, Solid State Commun. **6**, 163 (1968).
[18] S.G. Chou *et al.*, Solid State Commun. **11**, 277 (1972).